## PHYSICAL REVIEW B, VOLUME 65, 033403

## Electric-field distribution near current contacts of anisotropic materials

E. Slot and H. S. J. van der Zant

Department of Applied Sciences and DIMES, Delft University of Technology, Lorentzweg 1, 2628 CJ Delft, The Netherlands

## R. E. Thorne

Laboratory of Atomic and Solid State Physics, Clark Hall, Cornell University, Ithaca, New York 14853-2501 (Received 15 August 2001; published 13 December 2001)

We have measured the nonuniformity of the electric field near lateral current contacts of the charge-density-wave materials NbSe<sub>3</sub> and *o*-TaS<sub>3</sub>. In this contact geometry, the electric field increases considerably near a current contact. Fitting our data to an existing model yields values for the conduction anisotropy and a characteristic longitudinal length scale. This length scale is on the same order as the mesoscopic phenomena in charge-density-wave devices.

DOI: 10.1103/PhysRevB.65.033403 PACS number(s): 71.45.Lr, 72.15.Nj

Anisotropic conductors with a chainlike structure can undergo a phase transition to a charge-density-wave (CDW) state. Electrons condense into a collective state in which the charge density is periodically modulated. The CDW can slide through the crystal under the application of an electric field. However, defects in the crystal lattice pin the CDW at low fields and a threshold has to be overcome. The experimental study of CDW dynamics usually involves transport measurement along the chain direction. Electrical contact is most often made by connecting metal electrodes to the crystal at various positions on the top or bottom side (face) of the crystal or, more recently, by etching side contacts in the crystal itself. Most transport studies have been performed on samples with contact spacings of  $10~\mu m$  and larger.

Recently, interest has grown to study the mesoscopic CDW regime. 3,4 As the length scale for mesoscopic phenomena is on the order of microns in the longitudinal direction, it is essential to reduce contact spacings to this scale. Since both types of lateral contacts mentioned above apply current in the transverse direction, a region of nonuniform electric field exists in the vicinity of current contacts. This nonuniformity is known under the name "fringing effects." In previous experiments so far, measurements of fringing effects were limited by perturbing contacts and large contact separation.

In case of anisotropic materials, fringing effects are particularly pronounced. In such materials, the length scale over which fringing effects are important is  $\sqrt{A}$  times larger than in the isotropic case. Here, A is the anisotropy, which is the ratio of the conductivity along and perpendicular to the crystal length.

We have measured the electric field distribution on submicron length scales in the longitudinal direction. We find good agreement with existing models which indicate that fringing effects are important up to distances of  $t\sqrt{A}$  from the current contact, where t is the crystal thickness. From our data, we can deduce the corresponding A. We find it to be  $\sim 100$  for NbSe<sub>3</sub> and  $\sim 1000$  for o-TaS<sub>3</sub> at  $T = 120\,$  K. This is the first measurement of A in the crystallographic a axis of NbSe<sub>3</sub>. Our measurements are performed in the pinned state, so that our data concerns geometrical effects only, and does

not explore the complicated current dependent field profiles that develop when the CDW depins. <sup>5,6</sup>

Experiments are performed on crystals of NbSe<sub>3</sub> and o-TaS<sub>3</sub>. Both materials have an anisotropic chainlike structure and exhibit CDW states at low temperatures. NbSe<sub>3</sub> exhibits CDW transitions along the crystallographic b axis at  $T_{P1}$ =145 K and  $T_{P2}$ =59 K, while part of the conduction electrons remains uncondensed providing a metallic single-particle channel down to the lowest temperatures. The anisotropy of NbSe<sub>3</sub> is  $\sim$ 10–20 along the c axis<sup>7</sup> and estimated to be about 100 along the a axis. o-TaS<sub>3</sub> has a single transition at T=220 K below which all conduction electrons are condensed. The anisotropy of o-TaS<sub>3</sub> is typically 1000 and increases as the temperature is lowered.

Electrical contact is made by placing the crystals on arrays of 50 nm thick gold strips defined with electron-beam lithography. The width of the strips is 100 nm and the smallest separation is 300 nm. The narrow gold strips are used to inject current and to measure voltage. The position of the crystal is fixed by putting a drop of glue (ethyl-cellulose dissolved in ethyl-acetate) on top of it. In case of  $o\text{-TaS}_3$ , reliable Ohmic contacts are obtained by heating the substrate to  $120\text{--}130\,^{\circ}\text{C}$  up to an hour before putting the glue down. In case of NbSe3 crystals, heating the substrate to  $80\,^{\circ}\text{C}$  prevents the tiny crystals from floating in the glue solvent. The contact resistances at  $120\,^{\circ}\text{K}$  are on the order of  $2\,^{\circ}\text{K}\Omega$  for the NbSe3 samples and on the order of  $100\,^{\circ}\text{K}\Omega$  for the  $o\text{-TaS}_3$  samples.

Cross sections are deduced from measurements of the resistance R for different voltage probe spacings L at room temperature using resistivity values of 3  $\Omega \mu m$  for  $o\text{-TaS}_3$  (Ref. 9) and 2  $\Omega \mu m$  for NbSe<sub>3</sub>. We have also used Shapiro step measurements to determine the cross section. These measurements involve a combined dc and ac current, such that the narrow band noise frequency produced by CDW sliding mode locks to the external ac frequency. At 120 K, we found complete mode-locking on three samples, indicating high quality samples with flat surfaces. The cross sections deduced from Shapiro step measurement agree very well with those deduced from the resistance measurements at room temperature, see Table I. The width of the crystals is determined under an optical microscope, from which we can

TABLE I. Sample characteristics at 120 K. The cross sections S are deduced from room temperature resistance measurements; those from Shapiro step measurements are in brackets. No Shapiro step measurements have been performed on sample  $TaS_3$ -A. The values of  $t\sqrt{A}$  are deduced from the fit parameter Y in Eq. (2). From the thickness t of the crystals, values of the anisotropy A have been calculated. The error margins of A are also listed.

	$S(\mu \text{m}^2)$	$Y(10^{-3})$	$t\sqrt{A} \ (\mu \text{m})$	t (μm)	A
NbSe <sub>3</sub> -A	0.54 (0.54)	20	3.9	0.3	170±50
NbSe <sub>3</sub> -B	0.20 (0.21)	45	1.7	0.2	70±40
TaS <sub>3</sub> -A	1.52 (-)	2.8	28	0.7	1600±320
TaS <sub>3</sub> -B	0.48 (0.55)	12	6.5	0.3	470±235

deduce the thickness of the crystals. The error in t is estimated to be up to 25%.

Fringing effects were measured in two different  $o\text{-TaS}_3$  and two different NbSe<sub>3</sub> samples. These measurements regard the pinned state of the CDW and are performed in a four-probe current-biased configuration. The normal carrier conductivity of  $o\text{-TaS}_3$  is very low at low temperatures so that only measurements above 90 K are performed. NbSe<sub>3</sub> has a metallic channel down to liquid helium temperature and measurements have been performed for T > 25 K.

To measure fringing effects, we have deduced the linear resistance from current-voltage (IV) characteristics for several different current contact pairs. The current is injected from one of the narrow leads to a big gold pad on the side, 250 µm away to minimize the influence of fringing effects of the other contact. The IV characteristics are measured by oscillating the current by 1 mHz and measuring voltage at several distances d from the current contact. Here, d is the distance from the middle of the current contact to the middle of the voltage-probe pair (see Fig. 1). We have measured the voltage with probe pairs within current contacts, as well as beyond contacts. When the voltage probes are in the vicinity of one of the current contacts, the linear resistance is larger than the linear resistance when current is injected far away. This higher resistance due to the nonuniform electric field near the current contact is called the spreading resistance  $R_S$ .

Measurements of  $R_S$  of samples NbSe<sub>3</sub>-A and TaS<sub>3</sub>-A at 120 K are plotted in Fig. 1. A negative sign of the distance d represents the distance of the voltage probes beyond the current contacts. The spreading resistance is normalized to the linear resistance  $R_0$  when fringing effects are negligible, i.e., when the current is injected far from the two voltage probes (>200  $\mu$ m).

Figure 1 shows the current distribution near a current contact as determined from numerically solving the Laplace equation in two dimensions. The current is injected perpendicular to the length of the crystal. The electric field just above the contact is very high and the current even flows beyond the contact. As a consequence, the voltage probes beyond the current contacts detect a voltage of opposite sign and therefore the spreading resistance is negative beyond the contacts. However, the net current beyond contacts is zero.

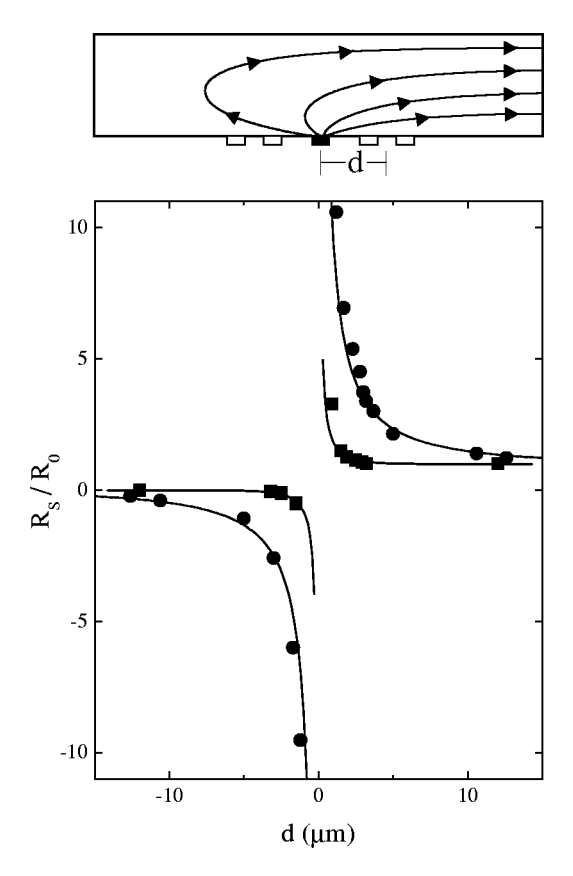


FIG. 1. Top: drawing of a side-view of a crystal with contacts at the bottom. The black contact is the current contact. Lines with arrows depict the numerically calculated paths of the current. The current is uniform at the right side of the drawing. Beyond the current contact on the left side, there is no net current, but at the bottom current flows in the opposite direction. The definition of d is also displayed. Bottom: the spreading resistance  $R_S$  as a function of the distance from the current contact of samples  $TaS_3$ -A (circles) and  $NbSe_3$ -A (squares) at 120 K. The solid lines are fits to Eq. (2).

We have fitted our data to analytical expressions obtained from Borodin *et al.*<sup>11</sup> who discuss the potential profile on the face of the crystal with lateral current contacts. They considered a metal electrode of width l with its middle at x=0. The other contact is at  $x=\infty$ . The potential U on the face of the crystal is

$$U(x) = -E \frac{t\sqrt{A}}{\pi} \operatorname{arc cosh} \left| \frac{\cosh\left(\frac{\pi l}{2t\sqrt{A}}\right) - \exp\left(\frac{\pi x}{t\sqrt{A}}\right)}{\sinh\left(\frac{\pi l}{2t\sqrt{A}}\right)} \right|,$$
(1)

where E is the electric field far from the current contact. A negative x denotes positions beyond current contacts. Our numerical calculations of the Laplace equation agree with the analytical potential profile on the face of the crystal of Eq. (1).

We use Eq. (1) to derive an estimate for the resistance ratio  $R_S/R_0$ , which is the quantity obtained from our measurements. Suppose the potential difference between two

voltage probes equals  $\Delta U$ . Then, for small probe spacing L, the potential difference  $\Delta U \approx (dU/dx)L$ , where dU/dx is the local electric field taken in the middle of two adjacent voltage probes. Then, the resistance ratio  $R_S/R_0$  equals (1/E)dU/dx. We introduce a dimensionless contact width  $Y = \pi l/4t\sqrt{A}$ . For narrow contacts  $(Y \ll 1)$ ,  $R_S/R_0$  can be expressed as

$$\left| \frac{R_S}{R_0} \right| = \frac{\exp(4Yx/l)}{2Y\sqrt{\left(\frac{1 - \exp(4Yx/l)}{2Y}\right)^2 - 1}}.$$
 (2)

The spreading resistance  $R_S$  approximates  $R_0$  when measuring far from the current contact, so that  $R_S/R_0$  goes to unity for  $x \rightarrow \infty$ . Beyond the current contact the spreading resistance is negative and goes to zero for  $x \rightarrow -\infty$ .

We have fitted our data with l = 100 nm and using Y as

the single fit parameter within and beyond contacts. Good fits were obtained on all samples in the temperature range studied. The values of Y obtained at 120 K are listed in Table I and all are consistent with the assumption  $Y \ll 1$ .

From the definition of Y the longitudinal length scale  $t\sqrt{A}$  and the anisotropy A are deduced. The anisotropy at 120 K of o-TaS<sub>3</sub> and NbSe<sub>3</sub> is on the order of  $10^3$  and  $10^2$ , respectively. The anisotropy of the thin samples seems to be underestimated. We have also determined Y at other temperatures and Y is approximately temperature independent. To get a better estimate of A(T), thicker crystals and a more accurate determination of the width are needed.

We acknowledge useful discussions with S.V. Zaĭtsev-Zotov and P.H. Kes. This work was supported by the Dutch Foundation for Fundamental Research on Matter (FOM). H.S.J.vd.Z. was supported by the Dutch Royal Academy of Arts and Sciences (KNAW).

<sup>&</sup>lt;sup>1</sup>G. Grüner, Rev. Mod. Phys. **60**, 1129 (1988).

<sup>&</sup>lt;sup>2</sup>S. G. Lemay, M. C. de Lind van Wijngaarden, T. L. Adelman, and R. E. Thorne, Phys. Rev. B 57, 12 781 (1998).

<sup>&</sup>lt;sup>3</sup>O. C. Mantel, F. Chalin, C. Dekker, H. S. J. van der Zant, Yu. I. Latyshev, B. Pannetier, and P. Monceau, Phys. Rev. Lett. 84, 538 (2000).

<sup>&</sup>lt;sup>4</sup>Yu. I. Latyshev, O. Laborde, P. Monceau, and S. Klaumünzer, Phys. Rev. Lett. **78**, 919 (1997).

<sup>&</sup>lt;sup>5</sup>T. L. Adelman, M. C. de Lind van Wijngaarden, S. V. Zaitsev-Zotov, D. DiCarlo, and R. E. Thorne, Phys. Rev. B 53, 1833 (1996).

<sup>&</sup>lt;sup>6</sup>M. E. Itkis, F. Ya. Nad, P. Monceau, and M. Renard, J. Phys.: Condens. Matter **5**, 4631 (1993).

<sup>&</sup>lt;sup>7</sup>N. P. Ong and J. W. Brill, Phys. Rev. B **18**, 5265 (1978).

<sup>&</sup>lt;sup>8</sup> Yu. I. Latyshev, Ya. S. Savitskaya, and V. V. Frolov, Pis'ma Zh. Éksp. Teor. Fiz. 38, 446 (1983) [JETP Lett. 38, 541 (1983)].

<sup>&</sup>lt;sup>9</sup>V. Ya. Pokrovskii, S. V. Zaitsev-Zotov, and P. Monceau, Phys. Rev. B 55, R13 377 (1997).

<sup>&</sup>lt;sup>10</sup>J. McCarten, D. A. DiCarlo, M. P. Maher, T. L. Adelman, and R. E. Thorne, Phys. Rev. B 46, 4456 (1992).

<sup>&</sup>lt;sup>11</sup>D. V. Borodin, S. V. Zaĭtsev-Zotov, and F. Ya. Nad, Sov. Phys. JETP **63**, 184 (1986).

<sup>&</sup>lt;sup>12</sup>The assumption that L is small is valid for all our samples. This has been checked by fitting our data to Eq. (1) using the exact  $\Delta U$  and comparing them to the fits to Eq. (2).